Growth Modes of InN (000-1) on GaN Buffer Layers on Sapphire

Bing Liu, Takeshi Kitajima*, Dongxue Chen, and Stephen R. Leone [a)]

Department of Chemistry and Department of Physics, and Lawrence Berkeley National Laboratory, University of California, Berkeley, CA 94720

---

* Permanent address: National Defense Academy of Japan, 1-10-20 Hashirimizu, Yokosuka 239-8686, Japan.

[a)] Electronic mail: srl@cchem.berkeley.edu

Abstract

In this work, using atomic force microscopy and scanning tunneling microscopy, we study the surface morphologies of epitaxial InN films grown by plasma-assisted molecular beam epitaxy with intervening GaN buffer layers on sapphire substrates. On smooth GaN buffer layers, nucleation and evolution of three-dimensional InN islands at various coverages and growth temperatures are investigated. The shapes of the InN islands are observed to be predominantly mesa-like with large flat (000-1) tops, which suggests a possible role of indium as a surfactant. Rough GaN buffer layers composed of dense small GaN islands are found to significantly improve uniform InN wetting of the substrates, on which atomically smooth InN films are obtained that show the characteristics of step-flow growth. Scanning tunneling microscopy imaging reveals the defect-mediated surface morphology of smooth InN films, including surface terminations of screw dislocations and a high density of shallow surface pits with depths less than 0.3 nm. The mechanisms of the three-dimensional island size and shape evolution and formation of defects on smooth surfaces are considered.

INTRODUCTION

InN is an important group-III nitride semiconductor. By varying the InN content, InGaN-based optoelectronic devices can have a wide range of working wavelengths from ultraviolet to red.[1] Among the group-III nitrides, InN recently has attracted more attention due to the newly-suggested small bandgap of 0.7 eV,[2] which potentially extends the spectral range covered by group-III nitrides to the near-infrared. In addition, InN has a very small electron effective mass and a high electron drift velocity,[3] which makes the material also promising in high-frequency electronic devices.

However, difficulties have been encountered due to the thermal instability of InN and the large lattice mismatches between InN and commonly used substrates (e.g., sapphire and silicon). During growth, the high equilibrium vapor pressure of nitrogen requires a high V/III flux ratio and a low growth temperature to suppress InN decomposition, which often results in unsatisfactory crystal quality and undesired three-dimensional (3D) rough surfaces. Several attempts to improve heteroepitaxial InN film quality and surface morphology have been reported. In molecular beam epitaxy (MBE), low temperature InN buffer layers [4] and InN intermediate layers [5] are used to achieve thick InN films with satisfactory room temperature carrier mobility and a low background carrier density. Bulk GaN,[6] epitaxial GaN [6, 7] and AlN films [6, 8] are also used by a few groups as templates for InN growth. One possible reason for the often-observed 3D rough surface of epitaxial InN is insufficient adatom surface diffusion due to the nitrogen-rich growth conditions, which is a well-known effect for GaN growth.[9] To overcome this difficulty, Lu et al. [10] studied migration-enhanced MBE of InN by alternately supplying indium vapor and nitrogen plasma to increase the adatom surface diffusion. However,

despite these efforts, the desired two-dimensional (2D) step-flow growth of InN is still rare.

Another reason for the 3D growth mode in the heteroepitaxy of InN is the lattice mismatch between InN and the substrates. In general, 3D islands can form during heteroepitaxy of lattice-mismatched materials via the Stranski-Krastanov (SK) or Volmer-Weber (VW) mechanisms to relieve the film stain. For fabrication of quantum dots in optoelectronic devices, these two growth modes have the advantage of forming nanometer-sized 3D islands by self-assembly. For InN/GaN heteroepitaxy, which involves a large lattice mismatch of 10%, it has been suggested that the growth of InN on GaN(0001) can follow the SK growth mode.[11] Ng et al.[11] studied the initial stage of MBE growth of InN on GaN(0001) surfaces and reported that under conditions of low growth temperatures and high nitrogen fluxes, strain relaxation via 3D island formation can start from the first monolayer (ML) of deposition, but 2D growth is favored under indium-rich conditions. However, systematic studies of the InN island size distribution [12] and island shape and aspect ratio, which are important to understand the evolution of 3D islands grown in the SK or VW modes, are still rare.

In this work, using plasma-assisted MBE, we investigate the growth modes of InN (000-1) on sapphire with GaN buffer layers. Using *ex-situ* atomic force microscopy (AFM) and *in-situ* scanning tunneling microscopy (STM), we examine in detail the size, shape, and aspect ratio of 3D InN islands grown on smooth GaN surfaces under conditions of various growth temperatures and coverages. We then explore the possibility of obtaining step-flow growth by using different types of GaN buffer layers. Smooth 2D InN films are achieved when using small dense GaN islands as a buffer layer, and the

surface morphology, including atomic steps and surface defects, are revealed by STM imaging.

EXPERIMENTS

The growth experiments are performed in a home-built MBE chamber with a base pressure of 10^{-8} Pa. Indium and gallium are evaporated from Knudson cells, and the beam fluxes are calibrated using a quartz crystal microbalance. An electron-cyclotron-resonance (ECR) plasma source is used for producing nitrogen ions (N_2^+ and N^+) and neutral radicals. Sample surface crystal structure and chemical composition are examined by low energy electron diffraction (LEED) and Auger electron spectroscopy (AES), respectively.

Sapphire wafers are cut into small pieces of 1 cm x 2 cm size and mounted on a tantalum sample holder. The back of the substrates are coated with a layer of titanium for efficient radiative sample heating. After degreasing in acetone and methanol and rinsing with de-ionized water, the sapphire substrate is further cleaned by an oxygen plasma in the sample load lock chamber for a few minutes to remove hydrocarbon contaminants. The substrate is then transferred to the growth chamber through vacuum. After outgassing at temperatures $\leq 800\ ^{o}C$ for a few hours, the LEED patterns of the substrate contain bright sharp spots with a six-fold symmetry, which confirms that the surface is clean and well-crystallized.

Growth experiments are started by first exposing the sapphire substrate at $720\ ^{o}C$ to the nitrogen plasma for 10 min to achieve nitridation. A layer of GaN is then grown as the template for the subsequent InN growth. For the growth of GaN, in general, a Ga/N

flux ratio at (or slightly above) one gives smooth GaN surfaces, while growth in the N-rich regime results in 3D rough surfaces. Our previous study of GaN MBE has enabled us to grow atomically flat GaN on relatively large scales (on the order of microns) at medium temperatures around 650 ^{o}C. Details of the GaN growth are reported elsewhere.[13] To study the 3D InN island formation, InN of 2-12 ML is deposited on this type of smooth GaN surface at temperatures between 400 ^{o}C and 480 ^{o}C under N-rich conditions. 3D GaN buffer layers are also used to improve the coalescence of InN islands. InN films up to 120 nm thick are grown on both smooth and rough GaN buffer layers. The estimated growth rate of InN is about 30 nm/hr. No metal droplets are observed by AFM and STM on the film surfaces, which confirms the N-rich growth conditions.

After growth, the sample temperature is lowered quickly to room temperature by switching off the sample heater. The sample can then be transferred through vacuum into a separate chamber with a base pressure of 10^{-7} Pa for STM imaging. A sample bias of ±2-4 V and a tunneling current of 0.1-0.3 nA are used. Although the sapphire substrates are insulators, we find that the conductivity of our unintentionally doped InN layers is sufficient to conduct the tunneling current, and electrical contacts are simply made (in vacuum) by applying metal clips to the film surfaces. The STM tips are etched from platinum/iridium alloy wires. Smooth InN film surfaces are examined by both *in situ* STM and *ex situ* AFM. 3D InN islands are mostly characterized by *ex situ* AFM. An algorithm is developed by the authors to analyze the island size and shape distributions.

The polarity of our MBE-grown InN films is probably N-polar (referred to as (000-1) in this paper). This is presumed from many previous reports that show MBE-

grown group-III nitrides on nitridized sapphire substrates are mostly N-polar.[14] Etching of our MBE-grown GaN films with KOH [14, 15] also confirms this.

RESULTS AND DISCUSSIONS

A. Growth on smooth GaN layers

Smooth GaN layers are first prepared by MBE growth at 650 ^{o}C. LEED patterns of the GaN surfaces contain bright sharp six-fold 1x1 spots. No reconstructions [16] or faceting spots [17] are observed. These LEED patterns indicate flat surfaces with no extra Ga. The substrate temperature is then lowered for the subsequent InN growth. Figures 1(a-c) show the AFM images of three samples of InN islands with estimated average coverages of 2, 6, and 12 ML, respectively, grown under N-rich conditions at 400 ^{o}C. (Note the different length scales in figure captions.) The corresponding distributions of island height and height-vs-area plots are displayed in Figs. (d-f) and Figs. (g-i), respectively. For the sample shown in Fig. 1(a), small islands with an average height of 0.7 nm and area of 400 nm^2 (see Fig. 1(g)) are observed. Note that the height of 0.7 nm is very close to the lattice constant c of wurtzite InN (0.6 nm), suggesting that these islands are two bi-layers (1 bi-layer=In+N=c/2) high.

With the coverage increased to 6 ML (Fig. 1(b, e, and h)), it is interesting to note that there are multiple peaks in the island height distribution. The average interval of 0.6 nm between these peaks is equivalent to the lattice constant c of wurtzite InN, which means that most islands contain even numbers of bi-layers. The distribution of the island lateral size (area) can be viewed from the height-vs-area plot of Fig. 1(h), where, on average, the island height increases with the island area.

When the coverage is increased to 12 ML, a significantly different island height distribution is observed, as shown in Fig. 1(f). Basically, from the height-vs-area plot of Fig. 1(i), it can be seen that the islands can be divided into two groups, as indicated by the two ellipses. For the group of smaller islands with heights between 2-4 nm, the relationship between the island heights and lateral sizes is similar to the case of 6 ML, i.e., the height increases with the area. The distribution of the island heights of this group can be fit by a Gaussian distribution, as shown in Fig. 1(f). For the group of larger islands, on average, instead of increasing with the lateral size, the island heights reach a plateau around 5.5 nm.

Based on the above observations, we consider possible mechanisms of InN island nucleation and growth at temperatures around 400 ^{o}C. First, from the height-vs-area plots, the average aspect ratio (height vs half width) of the islands at low coverages (2 ML and 6 ML) is estimated to be on the order of 1/10. This low aspect ratio means that the lateral growth of InN on GaN(000-1) is much faster than the vertical growth, despite the large lattice mismatch between InN and GaN. At the beginning of growth, InN basically nucleates as 2D islands (e.g, in Fig. 1(d), where the average island height is equivalent to one bi-layer of InN). With the coverage increased to 6 ML, 3D islands form, which provide strain relaxation, and the average island height slowly increases in 'quanta' of double bi-layer heights (which should help to preserve the stacking sequence along the [0001] direction of the wurtzite structure). The results for 12 ML InN (in particular, the height-vs-area plot of Fig. 1(i)) indicate that the vertical growth of islands slows down significantly for islands with lateral areas larger than 3000 nm^2, after which, lateral

growth dominates the island shape evolution. This change of the growth mode suggests a bimodal process for the InN islands on GaN(000-1).

Bimodal size distributions have been observed previously for islands grown in the SK mode for heteroepitaxy of other materials, e.g., Ge/Si.[17-19] Two major mechanisms can contribute to this phenomenon. First, smaller islands can coalesce to form larger islands. Second, at a critical size, single small islands can evolve into a different shape with a lower free energy through a phase transition.[19] For example, for Ge/Si(001),[18, 19] small Ge islands have shallow pyramid-like shapes with a low aspect ratio. Larger than a critical size, Ge islands take on a higher aspect ratio with steeper facets. For both types of Ge islands, the equilibrium island shape is determined by the balance between strain and the island surface energies. For InN islands, the plateau of the island height versus lateral size suggests a very low surface energy of InN(000-1), which favors a flat island shape with a large (000-1) face. Significant lateral growth of InN islands is also observed at higher temperatures, as introduced next.

Figures 2(a, b) are AFM images of 6 ML InN grown at 440 ^{o}C and 480 ^{o}C, respectively. The corresponding island height distributions and height-vs-area plots are displayed in Figs. 2(c, d) and Figs. 2(e, f), respectively. For the growth at 440 ^{o}C, compared with the growth results at 400 ^{o}C (Fig. 1(b, e)), the islands have a lower density and larger lateral sizes. Presumably the increased temperature alters the adatom mobility of surface diffusion, which causes the change in island density. However, the height distribution (Fig. 2(c)) does not change significantly; it also contains multiple peaks with an average interval of about 0.6 nm that is close to the lattice constant c of InN. The

height-vs-area plot (Fig. 2(e)) shows that the island height reaches a clear plateau at about 2.7 nm.

With the temperature increased to 480 ^{o}C, a multi-modal island height distribution is also observed, as shown by the height distribution and height-vs-area plot in Figs. 2(d, f), respectively. In particular, the several peaks in the height distribution generally correspond to the several groups of islands indicated by the ellipses in the height-vs-area plot, and the groups of islands with greater heights have smaller lateral sizes.

The above results can be explained partly by considering the balance between strain and island surface energy. In general, surface energy plays a critical role in determining the epitaxial growth mode. A well-known example is the use of surfactants (e.g., As [20]) to modify (lower) the surface energy of Ge(001) such that the usual SK growth mode of Ge/Si(001) can be changed to a 2D growth mode. However, for compound semiconductors, unreconstructed polar surfaces are usually unstable due to charge effects. For example, it is well-known that the InSb (111)A surfaces are stabilized by a 2x2 vacancy reconstruction which neutralizes the surface charge.[22] For 1x1 GaN(000-1), it has been suggested that an extra monolayer of Ga adatoms can stabilize the surface.[16] For InN, values for the surface energies of different crystal planes are currently not available. We speculate, though, that an indium adlayer may occur and play a role in lowering the InN(000-1) surface energy. In general, because the equilibrium vapor pressure of nitrogen over InN is higher than that over GaN by several orders of magnitude,[23] more nitrogen atoms are required for growth of InN. With the limited supply of nitrogen atoms produced by commonly used plasma sources (ECR or radio-frequency), a small amount of excess indium many exist on the surface due to

segregation, which effectively lowers the surface energy of InN(000-1). Therefore, it is possible that the vertical growth of islands at the high temperature of 480 ^{o}C is partly due to the enhanced desorption of indium, such that the growth is under more N-rich conditions, and excess indium is unavailable to stabilize the (000-1) surfaces. The separate groups of islands formed at 480 ^{o}C also suggests a temperature-activated change of the island shape, which is favorable to relax the strain by the smaller lateral sizes and increased heights (Fig. 2(f)).

From the above discussion, we expect that the effective low surface energy of InN(000-1) may lead to the formation of continuous 2D InN films by coalescence of the quasi-2D islands at medium temperatures around 440 ^{o}C. Similar methods have been applied in heteroepitaxy of a few materials to obtain continuous 2D films, for example, in the growth of InAsSb on GaAs(001) surfaces.[24] However, in our experiments on flat GaN surfaces, growth of InN up to 90 nm thick at 440 ^{o}C does not provide satisfactory continuous 2D films. An AFM image and a typical line profile of such an InN film are shown in Fig. 3. The film is composed of pillars with flat (000-1) tops separated by deep trenches. The line profile measurement (Fig. 3(b)) shows a dominating contact angle between 60^{o} and 70^{o} of the InN pillars with the substrate, which is close to the contact angle of the (10-11) plane with the basal plane. Extended growth up to 120 nm can not repair this type of morphology. One possible reason is the appearance of additional surface planes (e.g., (10-11)) that can balance the surface energy of (000-1). Another possible reason is defect formation, such as valleys and grooves often observed in epitaxial GaN films.[25, 13] Exploration of alternative ways of achieving continuous 2D InN films is introduced in the next section.

B. Growth of 2D InN films on 3D GaN buffer layers

In epitaxial growth of GaN, the use of 3D buffer layers of AlN or GaN grown at low temperatures have been shown to significantly improve the expitaxial GaN film quality and surface morphology.[26] Following these examples, we explore the possibility of obtaining smooth 2D InN films by using GaN buffer layers composed of 3D GaN islands.

Figures 4(a-c) show large scale (5 μm x 5 μm) AFM images of 60 nm InN grown on 3D GaN buffer layers. The growth temperature of InN is 440 ^{o}C for all three samples, and the growth temperatures of the GaN buffer layers are 440 ^{o}C, 480 ^{o}C, and 520 ^{o}C for the samples in Fig. 4(a-c), respectively. Compared with Figure 3(a), where a 2D smooth GaN template is used for the InN growth, the improvement of InN wetting of the substrate by using 3D GaN buffer layers is apparent. In particular, the surface shown in Fig 4(c) is composed of spiral growth hillocks and shallow valleys, which is very close to previously-reported good surface qualities of MBE-grown GaN films.[27] The inset in Fig. 4(c) is the corresponding InN LEED pattern. The bright 1x1 spots and the low background confirm the surface crystal quality. No satellite spots of reconstruction are observed, which confirms the N-rich growth. Figure 4(d) shows an AFM image of the typical 3D islands of a GaN buffer layer grown under similar conditions as those used for the buffer layer in the InN sample shown in Fig. 4(c). Compared with the poor wetting of InN on smooth GaN surfaces, as exemplified in Fig. 3, it is anticipated that one role of the dense and small 3D GaN islands of the GaN buffer layer is to serve as nucleation centers for InN growth so that InN can quickly wet the entire substrate. Thus the formation of trenches such as those shown in Fig. 3(a) can be avoided. In addition, a 3D

GaN buffer layer is more deformable (both laterally and vertically) than a 2D GaN layer, allowing better stain relaxation for the InN layers.

The large numbers of surface pits shown in Fig. 4(a) and 4(b) are probably surface terminations of threading dislocations,[27] which is discussed further below. Note that the number of surface pits decreases and the overall surface quality improves with increasing growth temperature of GaN buffer layers from Fig. 4(a) to 4(c), suggesting a sensitive dependence of the final film quality on the GaN buffer layer growth conditions. This can be attributed to the improved crystal quality of the 3D GaN islands with increasing growth temperatures.

Details of the 2D InN films are revealed by *in situ* STM imaging, as shown in Figs. 5(a-c). The sample is grown under similar conditions to those used for the sample in Fig. 4(c). In Fig. 5(a), several atomic steps can be seen emanating from a surface pit, suggesting that the pit is related to a screw type dislocation. According to the early theoretical work by Frank,[28] atomic steps generated by screw dislocations can enhance the step-flow growth by spiral growth processes. (Note that in Fig. 5(a), there are no islands on the terraces, which is a typical result of step-flow growth.) This mechanism largely contributes to the hill and valley morphology shown in Fig. 4(c). Line profile measurements of our STM images show predominant step heights of 0.3 nm and 0.6 nm, which correspond to single and double bi-layer steps, respectively.

By counting the number of steps emanating from a defect, the strength of the associated threading dislocation can be estimated. For example, the few defects shown in Fig. 5(b) all generate pairs of single steps, which implies Burgers vectors of [0001] or its multiples.

An extremely high density of very shallow surface pits also exists on the surface of the InN sample, as apparent in Fig. 5(b) and 5(c). The depths of these pits are between 0.1-0.25 nm, shallower than a single bi-layer. Because changing the polarity of the bias voltage does not affect the appearance of the pits, the shallow pits must be morphological defects. Regarding the origin of these defects, we exclude the possibility that these are surface endings of edge dislocations, which usually result in deeper surface pits and are only apparent at high temperatures.[29] Considering the thermal instability of InN in vacuum and the low growth rate of our experiments, it is possible that these pits are the result of InN decomposition. More investigation is needed to better understand the formation of these defects.

We also perform scanning tunneling spectroscopy (STS) measurements, where the tunneling engagement is set at 1.1 nA at 2-3 V. An area-averaged I(V) curve and a normalized conductivity curve are displayed in Fig. 5(d) and 5(e), respectively, which show a typical metallic behavior [30] instead of a bandgap. This can be evidence of the possible indium surface segregation, as discussed earlier. Incorporation of a high density of background doping (n-type for InN [6]) can also result in metallic behaviors of the films. More investigation is needed to further understand this.

CONCLUSIONS

In summary, we have performed systematic studies of the surface morphologies resulting from 3D and 2D growth modes of InN (000-1) grown on sapphire substrates with intervening smooth and 3D GaN buffer layers, respectively. Analysis of the results for growth of 2-12 ML InN islands on smooth GaN surfaces at temperatures between 400

^{o}C to 480 ^{o}C reveals predominant flat island shapes with large (000-1) faces, which suggests an effective low surface energy of InN(000-1). One possible explanation is proposed to be the self-surfactant effect of indium surface segregation. To improve the uniformity of wetting of InN on the substrates, rough GaN buffer layers composed of dense small 3D GaN islands are used and step-flow growth of InN is achieved, but with screw-dislocation-enhanced spiral growth. STM imaging reveals the single and double atomic steps and terminations of screw dislocations. A large number of shallow surface pits is also observed, which possibly comes from InN decomposition. STS measurements also suggest metallic behavior of the InN surfaces.

ACKNOWLEDGMENTS

The authors are grateful for the financial support from the Department of Energy (Contract No. DE-AC03-76SF00098) and also for the National Institute of Standards and Technology for loan of part of the experimental equipment.

References

[1] J. I. Pankove and T. D. Moustakas ed., *Gallium Nitride (GaN) I*, Semiconductor and Semimetals, Vol **50**, (Academic Press, San Diego, 1998), pp 241.

[2] J. Wu et al., Appl. Phys. Lett. **80**, 3967 (2002).

[3] S. K. O'Leary, B. E. Foutz, M. S. Shur, U. V. Bhapkar, L. F. Eastman, J. Appl. Phys. **83**, 826 (1998).

[4] V. V. Mamutin et al., Phys. Status Solidi A **176**, 247 (1999).

[5] Y. Saito et al., J. Cryst. Growth **237**, 1017 (2002).

[6] For example, see the review by A. G. Bhuiyan, A. Hashimoto, and A. Yamamoto, J. Appl. Phys. **94**, 2779 (2003).

[7] R. A. Oliver et al., Surf. Sci. **532**, 806 (2003).

[8] H. Lu et. al., Appl. Phys. Lett. **79**, 1489 (2001).

[9] T. Zywietz, J. Neugebauer, and M. Scheffler, Appl. Phys. Lett. **73**, 487 (1998).

[10] H. Lu et al., Appl. Phys. Lett. **77**, 2458 (2000).

[11] Y. F. Ng, et al., Appl. Phys. Lett. **81**, 3960 (2002).

[12] Y. G. Cao et al., Appl. Phys. Lett. **83**, 5157 (2003).

[13] B. Liu, T. Kitajima, T. H. Zhang, C. Borca, and S. R. Leone, J. Appl. Phys, in press.

[14] A. R. Smith et al., Appl. Phys. Lett. **72**, 2114 (1998).

[15] M. Seelmann-Eggebert et al., Appl. Phys. Lett. **71**, 2635 (1997).

[16] A. R. Smith, R. M. Feenstra, D. W. Greve, J. Neugebauer, and J. E. Northrup, Phys. Rev. Lett. **79**, 3934.

[17] S. Sloboshanin et al., Surf. Sci. **427**, 250 (1999), and references therein.

[18] Y. W. Mo, D. E. Savage, B. S. Swartzentruber, and M. G. Lagally, Phys. Rev. Lett. **65**, 1020 (1990).

[19] G. Medeiros-Ribeiro, A. M. Bratkovski, T. I. Kamins, D. A. A. Ohlberg, and R. S. Williams, Science **279**, 353 (1998).

[20] F. M. Ross, R. M. Tromp, and M. C. Reuter, Science **286**, 1931 (1999) and references therein.

[21] R. M. Tromp and M. C. Reuter, Phys. Rev. Lett. **68**, 954 (1992).

[22] J. Bohr et al., Phys. Rev. Lett. **54**, 1275 (1985).

[23] For example, see J. I. Pankove and T. D. Moustakas ed., *Gallium Nitride (GaN) I*, Semiconductor and Semimetals, Vol **50**, (Academic Press, San Diego, 1998), pp127.

[24] T. P. Pearsall ed. *Strained-Layer Superlattices: Materials Science and Technology*, Semiconductor and Semimetals Vol **33**, (Academic Press, San Diego, 1991), pp22-25.

[25] K. H. Ploog, O. Brandt, R. Mauralidharan, A. Thamm, and P. Waltereit, J. Vac. Sci. Technol. B **18**, 2290 (2000).

[26] J. I. Pankove and T. D. Moustakas ed., *Gallium Nitride (GaN) I*, Semiconductor and Semimetals, Vol **50**, (Academic Press, San Diego, 1998), pp 23.

[27] B. Heying et al., J. Appl. Phys. **85**, 6470 (1999).

[28] F. C. Frank, Acta Crystallorgr. **4**, 497 (1951).

[29] S. Vezian, J. Massies, F. Semond, N. Grandjean, and P. Vennegues, Phys. Rev. B **61**, 7618 (2000).

[30] D. A. Bonnell ed. Scanning Tunneling Microscopy and Spectroscopy, (VCH Publishers, Inc. New York, 1993), pp 176.

Figure captions

Fig. 1. (a-c): AFM images of InN islands of 2, 6, and 12 ML grown at 400 ^{o}C on smooth GaN layers. Image sizes are 0.5x0.5 μm^2 for (a) and 2x2 μm^2 for (b) and (c). Black and white contrasts are 10 nm for all three images. (d-f) and (g-i): Corresponding island height distributions and height-vs-area plots. Vertical dotted lines in the height distribution (e) indicate the positions of the peaks; and the corresponding heights are indicated by the horizontal dotted lines in the height-vs-area plot (h). Ellipses in (i) indicate difference heigh-area relations. Also note the different x axis scales in (d-i).

Fig. 2. (a, b): AFM images of 6 ML InN islands grown at 440 ^{o}C and 480 ^{o}C, respectively. Image size and black and white contrast are 2x2 μm^2 and 10 nm, respectively, for both images. (c, d) and (e, f): Corresponding island height distributions and height-vs-area plots. Explanations of the dotted lines in (c) and (e) and the ellipses in (f) are similar to those in Fig.1 (e), (h), and (i), respectively.

Fig. 3. (a): AFM image of 90 nm InN film grown on a smooth GaN layer. Image size is 5x5 μm^2. Black and white contrast is 200 nm. (b): A typical line profile of the sample.

Fig. 4. (a-c): AFM images of 60 nm InN grown at 440 ^{o}C on rough GaN buffer layers composed of small 3D GaN islands. Inset of (c) is a LEED pattern taken with an electron beam voltage of 93 eV. The corresponding growth temperatures of the GaN buffer layers are 440 ^{o}C, 480 ^{o}C, and 520 ^{o}C. (d): 3D GaN islands grown at 520 ^{o}C. Image sizes are

5x5 μm^2 for (a-c) and 2x2 μm^2 for (d). Black and white contrasts are 20 nm for (a-c) and 10 nm for (d).

Fig. 5. (a-c): STM images of a 2D InN film. Images sizes are 150 nm x150 nm for (a) and (b) and 30 nm x 30 nm for (c). Bias voltages are -3 V for (a) and (b) and +2.7 V for (c). Tunneling current is 0.2 nA for all three images. (d) and (e) show an area-averaged I(V) curve and normalized conductivity curve of a scanning tunneling spectroscopy measurement, respectively.

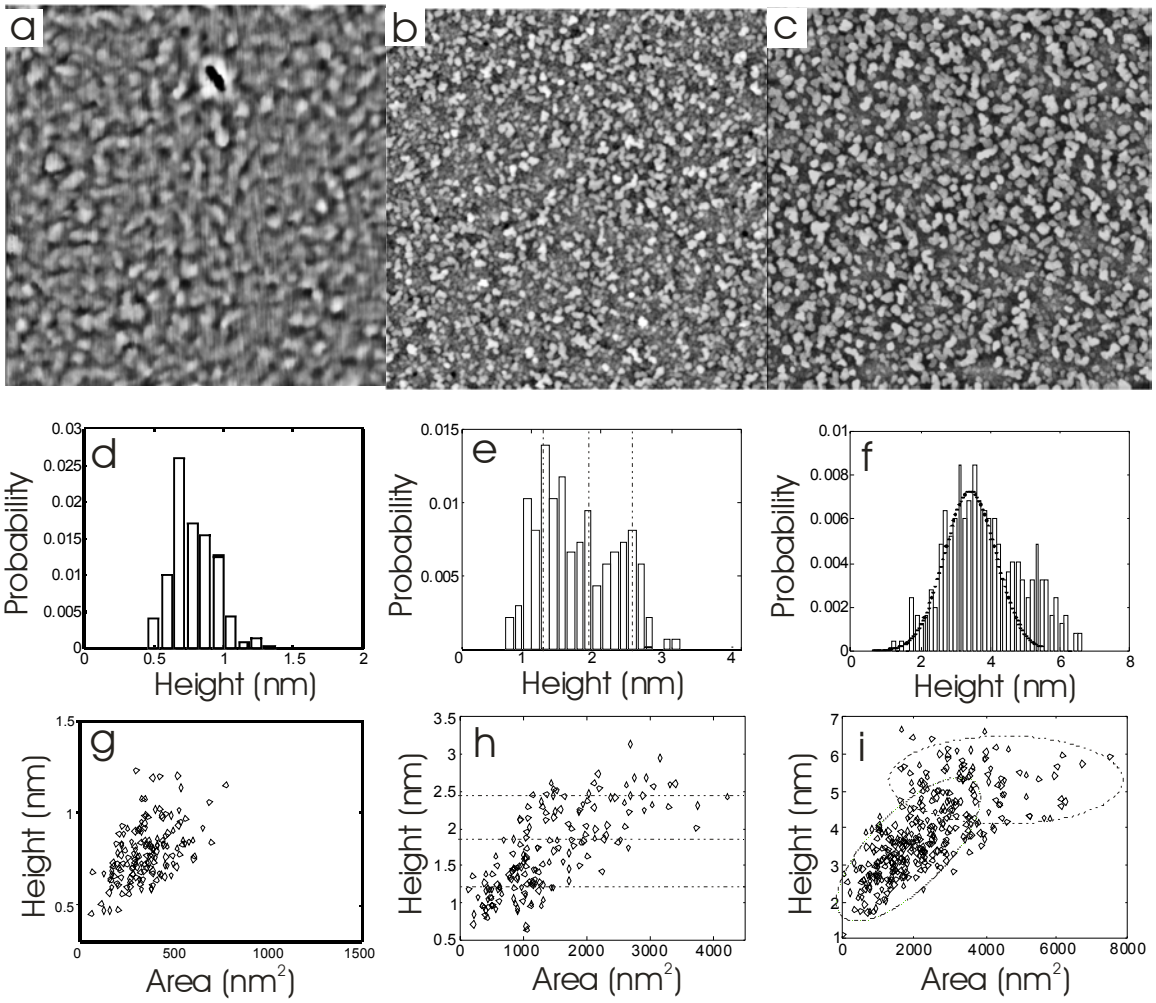

Figure 1. B. Liu et al.

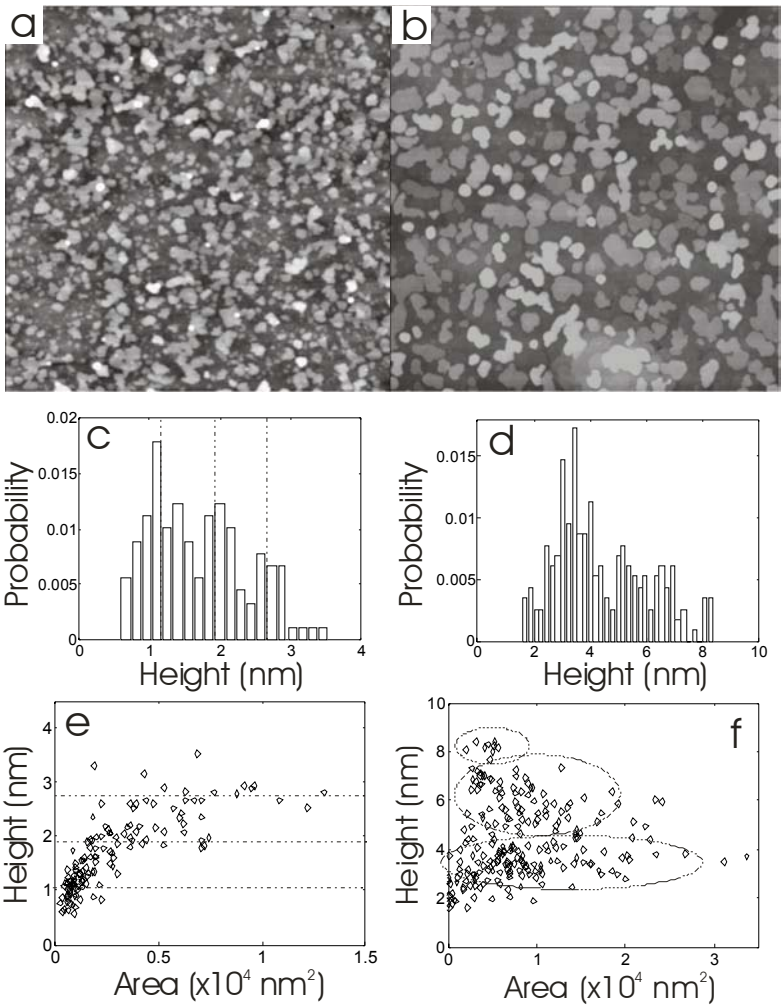

Figure 2. B. Liu et al.

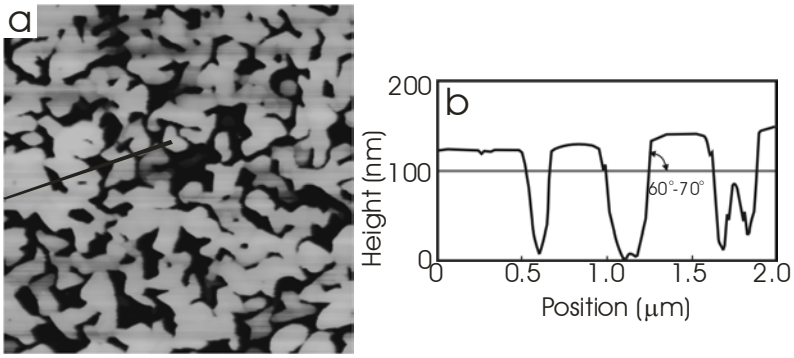

Figure 3. B. Liu et al.

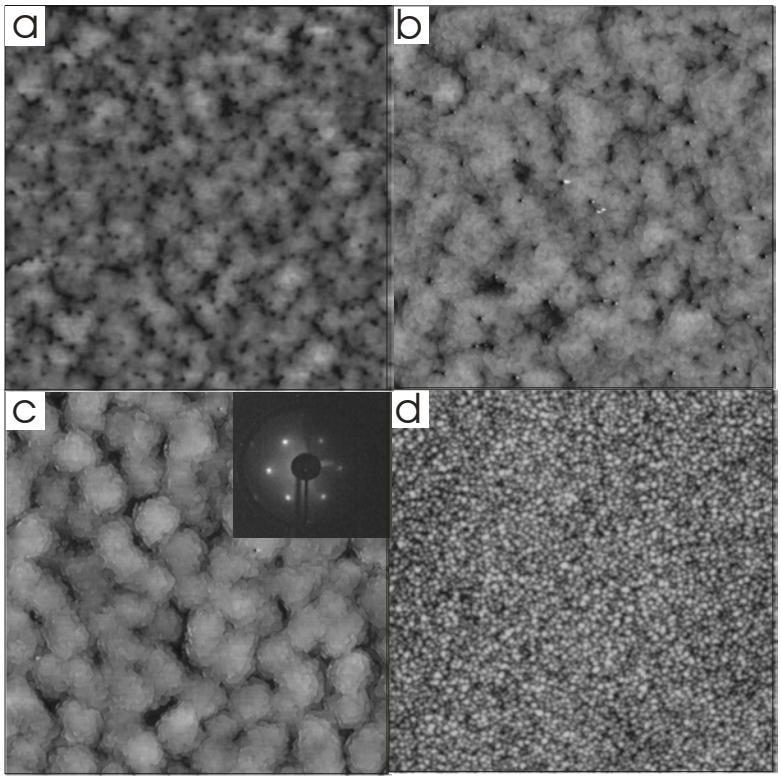

Figure 4. B. Liu et al.

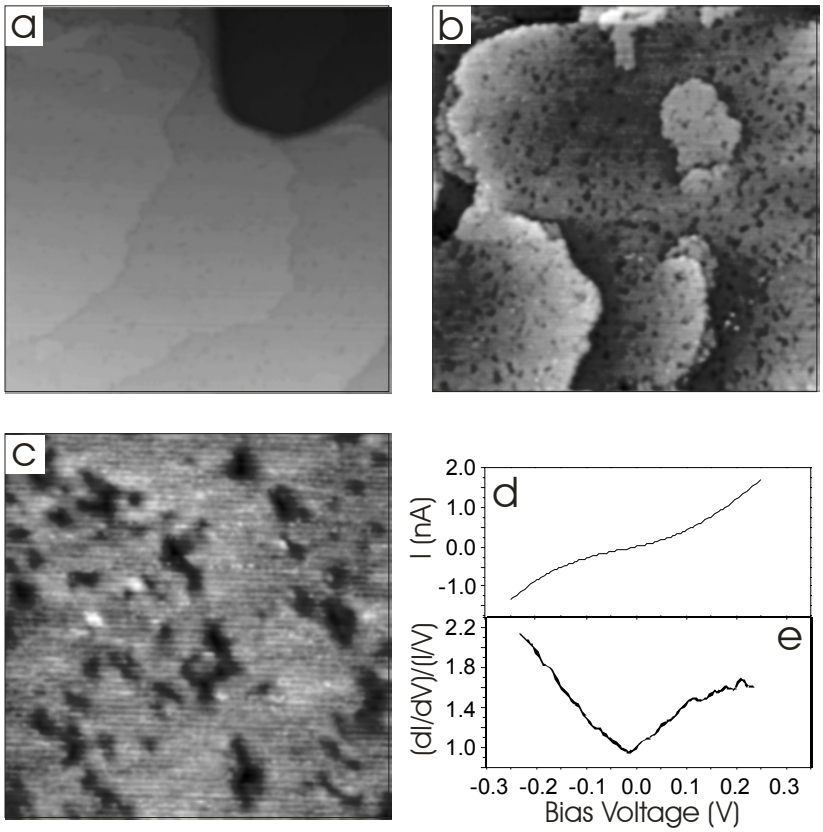

Figure 5. B. Liu et al.